Frequency-Time Behavior of Artificially Stimulated VLF Emissions

G. S. STILES AND R. A. HELLIWELL

Radioscience Laboratory, Stanford University, Stanford, California 94305

Artificially stimulated VLF emissions (ASE's) are emissions triggered in the magnetosphere by the whistler mode signals from VLF transmitters. These emissions may be separated into two classes, rising and falling, depending on whether the final value of df/dt is positive or negative. Several hundred ASE's triggered by three transmitters (NAA, Maine, 14.7 kHz, 1 MW; Omega, New York, 10.2 kHz, 100 W; Siple station, Antarctica, 5.5 kHz, 400 W) have been analyzed using the fast Fourier transform with a filter spacing of 25 Hz and an effective filter width of about 45 Hz. The study was limited to the initial frequency-time behavior of ASE's. Averages taken over many events reveal that both rising and falling tones show the same initial behavior. The emissions begin at the frequency of the triggering signal rather than at an offset frequency, as has previously been reported. Both tones initially rise in frequency, falling tones reversing slope at a point 25–300 Hz above the triggering signal. The slope of rising tones, particularly those triggered by NAA, often abruptly levels off in this same frequency range; as a result, a short (~40 ms) plateau is formed that precedes the final rising phase. The initial frequency offset commonly observed in individual events appears to result from the frequent coincidence with this plateau of a peak in amplitude. Emissions stimulated by all three transmitters show essentially the same features; this finding indicates that their frequency behavior does not depend strongly on transmitter power. The process appears to be asymmetric in frequency; no evidence of initial growth below the triggering frequency has been found.

Artificially stimulated VLF emissions (ASE's) represent only one of the many diverse forms of discrete VLF emissions. Since they are triggered by signals from VLF transmitters, however, they have the potential of becoming a valuable controlled tool for the study of the magnetosphere.

The triggering of emissions by VLF transmitters (NPG, 18.6 kHz, $\sim 2 \times 10^5$ W; NAA, 14.7 kHz, $\sim 10^6$ W) was first reported by *Helliwell et al.* [1964]. *Kimura* [1968] extended the known range of the phenomenon to lower frequencies (10.2 kHz) and lower power (~100 W) with his observation that the New York Omega transmitter also stimulated emissions. In 1973 the frequency range was lowered further when the Stanford transmitter at Siple station, Antarctica, was employed in triggering emissions in the band from 2.5 to 7 kHz [*Helliwell and Katsufrakis,* 1974].

Investigations subsequent to the original discoveries have revealed several intriguing features of ASE's. First, Morse dashes (150 ms long) trigger ASE's much more frequently than do Morse dots (50 ms) [*Helliwell et al.,* 1964; *Helliwell,* 1965; *Lasch,* 1969]. Second, triggering tends to occur most often when the transmitted frequency is within a few percent of one half the minimum gyrofrequency along the whistler mode path [*Carpenter,* 1968; *Carpenter et al.,* 1969]. Third, the emissions often appear (misleadingly, as will be seen) to begin at a point offset above the frequency of the triggering signal by several hundred hertz [*Helliwell,* 1967; *Kimura,* 1967; *Lee,* 1968]. Additional features of ASE's, including occurrence statistics, may be found in the work of *Helliwell* [1965], *Kimura* [1967, 1968], and *Lee* [1968].

Several theories (reviewed by *Kimura* [1967] and *Gendrin* [1972]) based upon the interaction of the triggering signal with gyroresonant electrons have been proposed to account for the existence of the emissions. Proper use of these theories in the study of the magnetosphere requires that the important features of ASE's, such as growth rates and frequency-time behavior, be determined more precisely than in the past. A computer program to provide improved spectral resolution of ASE's, described in the following section, has been developed at Stanford. This paper will present results concerning the initial frequency-time behavior of ASE's. Growth rates are currently being studied and will be covered in a later paper. Future work will investigate long-term amplitude and frequency behavior and attempt to ascertain the factors controlling the evolution of triggered emissions.

ANALYSIS PROCEDURE

The primary purpose of the analysis is to define as accurately as possible the characteristics of triggered emissions. To accomplish this goal, we have developed an economical procedure of improved accuracy based upon the fast Fourier transform [*Bergland,* 1969].

The analysis procedure is outlined in the block diagram of Figure 1. The data selected for study are usually in the form of broad band (0–25 kHz) analog recordings. Since we are most often interested in only a small portion of the VLF spectrum (e.g., a 2-kHz band centered on NAA at 14.7 kHz), we first pass the broad band signal through a band-pass translator. This device filters out the desired 2.1-kHz portion of the spectrum and translates it down to the range from 0.5 to 2.6 kHz. This step not only removes unwanted signals but also results in a considerable saving in computer time. For fixed resolution, computation time is roughly proportional to the bandwidth of the signal analyzed.

The filtered and translated signal is then sampled at a rate of 6.4 kHz by an analog-digital (A-D) converter. This sampling rate, when it is coupled with the steep skirts of the band-pass filter, is adequate to prevent significant aliasing of unwanted signals. The 14-bit range of the A-D converter results in a quantization step size that is more than 60 dB below typical signal levels. The digital output, typically representing several minutes of analog data, is stored on magnetic tape.

These data are then Fourier analyzed by using a modified version of a program by *Cousins* [1971]. This program breaks the data into small segments whose length is chosen to provide the desired resolution in frequency and time. The amount of overlap in time between successive segments may also be

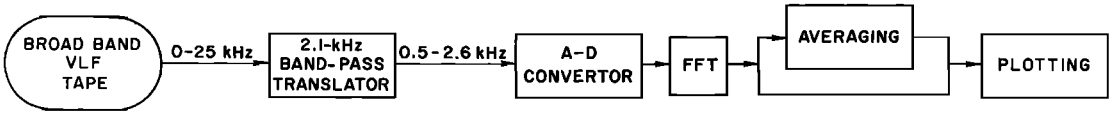

Fig. 1. A block diagram of the digital spectral analysis procedure. The data may or may not be averaged prior to plotting.

chosen. The data discussed in this paper were processed with a segment length of 40 ms and a 2 : 1 overlap in time between successive segments; this procedure yielded spectra spaced by 20 ms with alternate spectra being totally independent.

After the desired segment has been read into the computer, it is first multiplied by a weighting function (Hamming) to minimize the effects of leakage [*Bergland*, 1969]. The product is then fast Fourier transformed (FFT), and the resulting amplitude spectrum is stored as a complete record on a second tape. This procedure is iterated (typically several thousand times) until the analysis is complete.

The next step consists in using a line printer to make a combined frequency and amplitude versus time plot of all the spectral records from a single run; this provides 'quick look' information and allows individual events to be accurately located. If a more detailed display is desired, selected events may then be plotted by using an amplitude scan (or A scan) as shown in Figure 2.

At the top of this figure is a schematic illustration of the process we are studying; it is typical of a spectrogram that might be made from data recorded at Eights station, Antarctica. The subionospheric (SI) component of the Morse dash is received at a time designated as 0.0 s. Several tenths of a second later, depending upon the delay, the whistler mode (WM) component of the dash is received. The triggered emission typically appears after another 70–160 ms.

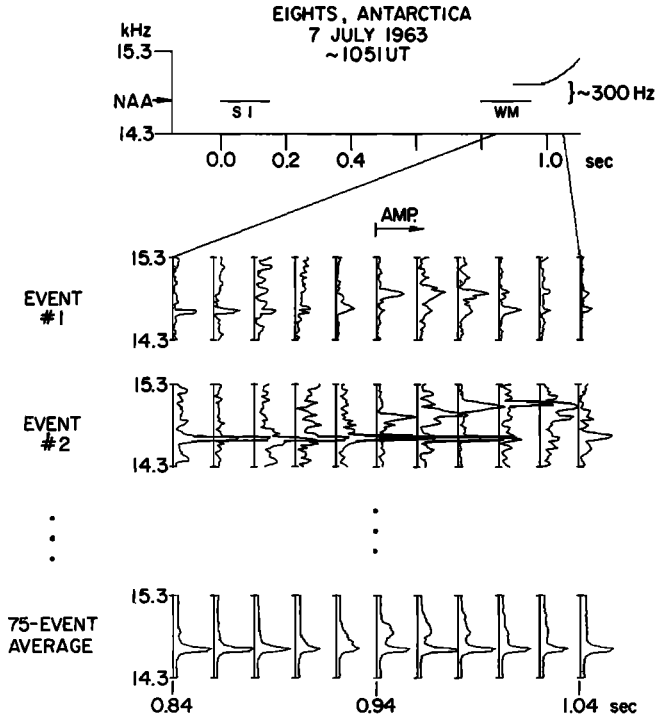

Fig. 2. (Top) Schematic illustration of an ASE as observed at the receiver. The triggering dash is received via the SI path approximately 0.8 s before the WM component and the triggered emission arrive. (Middle) Digital spectra of a portion of two events from July 7, 1963. The jaggedness of the spectra is caused by spherics. (Bottom) Average of the digital spectra of 75 ASE's from July 7, 1963. The presence of the emission at 0.9 and 0.92 s can now clearly be seen.

The middle portion of the figure shows the A scans for two events of July 7, 1963. Each trace, representing one spectral record, displays amplitude, increasing to the right, as a function of frequency from 14.3 to 15.3 kHz. Successive records are spaced by 20 ms. The prominent peaks at 14.7 kHz are the combined SI and WM signals from NAA. Emissions appear in the center of the plots approximately 250 Hz above NAA.

If we attempt to examine closely the initial appearance of the two emissions, we can see the problem inherent in working with individual events: details are often masked by the strong and characteristically jagged spectra of atmospheric lightning impulses (spherics).

Averaging, the last major step in the procedure, serves to minimize this interference. (Averaging also greatly improves the stability of the spectral measurements [*Welch*, 1967; *Hinich and Clay*, 1968].) Numbered records of the line printer plot are used to select the individual events to be averaged and to assure that they are correctly aligned with respect to time. The records from the selected events are then combined, and the resulting spectra are plotted, as is shown in the bottom portion of Figure 2. The improvement is evident immediately: the jagged spherics has been reduced to a uniform background about 15 dB below the level of the transmitted signal. This reduction allows much more detail to be seen in the region containing the onset of the emission. The averaging process also performs another useful function, that of identifying the repeatable and nonrepeatable features of the ASE's. In the bottom portion of Figure 2, for instance, the average triggered emission is fairly strong at 0.94 s; this finding indicates that the frequency at that time varies little from event to event. Following this peak, however, the average emission dies out rather rapidly; this behavior reflects the fact that individual events may vary considerably in their later behavior (as may be seen in events 1 and 2).

The details of this average (and others) will be discussed more fully in the next section. First, however, we shall comment briefly on the resolutions to be expected with this technique.

For the results given in this paper, each transform is performed over 40 ms of data. Before the segment of data is actually transformed, it is multiplied by a weighting function that has a half width of 20 ms. Successive transforms are spaced by 20 ms. This procedure results in a resolution in time that is approximately 30 ms.

Since 40 ms of data are transformed at one time, spectral estimates are obtained at integral multiples of 25 Hz; this is the equivalent filter spacing. The bandwidth of each filter, which is determined by the width of the weighting function, is approximately 45 Hz. These parameters yield a resolution in frequency of about 50 Hz; thus two equal amplitude signals spaced by 50 Hz will be reported as separate peaks if they are well above the background noise.

Since the filter spacing is 25 Hz, rough frequency

measurements of relatively narrow band signals may be made to within ±12.5 Hz. If the signal may be assumed to be nearly monochromatic, finer measurements (depending again on the noise) may be made by considering the amplitudes of the spectral points [*Rife and Vincent,* 1970]. The assumption of the presence of one monochromatic signal also allows some improvement in the resolution stated above. Since the spectral shape of such a signal is known, the presence of an additional signal within 50 Hz (or any departures from monochromaticity) may be inferred from changes in the shape of the spectrum. Such an inference will be discussed in the next section in connection with the initial appearance of triggered emissions.

RESULTS

The principal new result of the present work is that ASE's appear to begin at the frequency of the triggering signal. (This is in contrast to previous reports [*Kimura,* 1967; *Lee,* 1968] that indicated that the emissions begin at a frequency offset above or below the triggering signal by several hundred hertz.) This result immediately presents a problem in terminology; since the emission is apparently continuous with the (possibly amplified) triggering WM signal, it is unclear which part to call the triggering signal and which to call the emission. In this paper we shall refer to the unamplified signal from the transmitter as the triggering or injected signal. Any other signals, including additional signals at the transmitter frequency, will be referred to as emissions. The presence of an additional signal at (or very near) the transmitter frequency may be detected either by its persistence beyond the known duration of the triggering pulse or by the observation of a significant increase in its amplitude above that of the triggering signal.

The first spectra to be illustrated are emissions triggered by NAA during July 1963. The NAA transmitter, which radiates approximately one megawatt, is located at Cutler, Maine ($L \sim 3.2$), and during the period of observation was operating at 14.7 kHz. The emissions were recorded at Eights station, Antarctica ($L \sim 5.2$).

A schematic representation of the transmitted and received signals is shown in Figure 3; the frequency-time diagrams represent spectrograms of data that might be recorded at a northern hemisphere station and at Eights. The signal transmitted by NAA usually consists of nearly continuous Morse code traffic, as is shown in the top record. The transmitted signal then propagates to Eights via two paths, the SI and the magnetospheric or WM path. The signal traveling the SI path reaches the receiver after approximately a 30-ms delay; the WM delay varies with conditions but is typically 0.5–1.0 s. The composite received signal is shown in the Eights record. The various shadings indicate the possible combinations of received signals.

One of the main problems in analyzing emissions triggered by NAA is immediately apparent from the figure: the WM from one Morse character and the SI component of a subsequently transmitted character often overlap at the receiver. This makes it nearly impossible to obtain accurate amplitude measurements of the WM signal. Frequency measurements are not hampered, however, but are actually improved, since the presence of the overlapping SI signal provides a nearly continuous frequency reference for the analysis system. Nor does the overlap interfere with the timing necessary for computing averages. The leading edge of the SI pulse is typically easy to locate with the aid of a northern hemisphere record; since the WM delay is expected to vary little over a 1- or 2-min period, the SI pulse may then be used as a time reference.

In Figure 4 are presented spectral averages of NAA triggered emissions recorded at Eights on three days in June and July 1963; each set is accompanied by a short analog spectrogram showing several of the events contained in the average. The scales are linear in wave amplitude, and the time reference (0.0 s) is taken as the leading edge of the received SI dash that triggered each emission. Each trace shows the fairly uniform background level that results from averaging over many spherics. The prominent peak at 14.7 kHz is the average of the overlapping SI and WM components of the transmitted signal. The analog spectra demonstrate that the final frequency-time behavior of the emissions can vary considerably from event to event in a given run.

The most prominent feature in the averages outside of 14.7 kHz is the peak located several hundred hertz higher in the approximate center of each data set. This peak is located at the time and frequency corresponding to the origin of the emissions as determined from an examination of either the analog spectra or of individual digitally processed events (see, for example, Figure 2). The fact that this initial peak is fairly well defined in the averages indicates that its location in frequency and time is quite repeatable from event to event. In the top two cases the peak remains centered at nearly the same frequency for about 40 ms; as a result, a short plateau is formed. Following this peak the average emission broadens and dies out rather quickly; this is caused not by the demise of individual events but by the variability of their final behavior from event to event as shown in the analog spectra.

The repeatability of the initial appearance is emphasized in Figure 5. The maximum amplitude of the ASE's typically occurs near the front of the plateau. The histograms of the time and frequency of the maximum show that there is very little spread, in a given run, in time and only little more in frequency. The spread in time could in fact be caused by the 20-ms uncertainty in the measurements. (The histograms of Figure 5 contain fewer events than the spectral averages of Figure 4 because spherics and overlapping emissions occasionally make it difficult to locate accurately the maximum amplitude of an individual emission.)

It should be remembered that the time origin of these plots is taken as the leading edge of the SI component of the triggering dash. It would be more valuable theoretically to know the time delay relative to the leading edge of the triggering WM

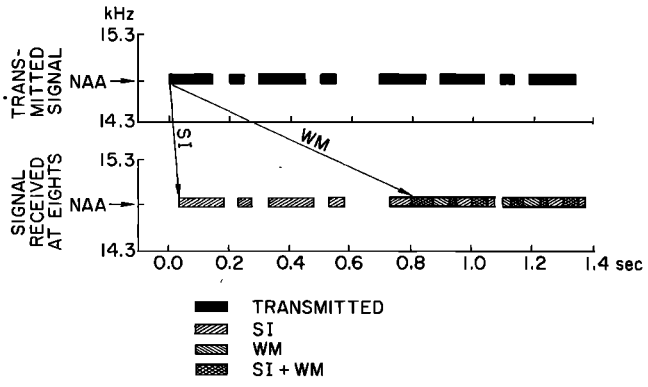

Fig. 3. A schematic representation of the signal transmitted from NAA and received at Eights station, Antarctica. It is assumed that no signal was transmitted prior to 0.0 s. Note the difficulty in identifying the overlapped SI and WM signals.

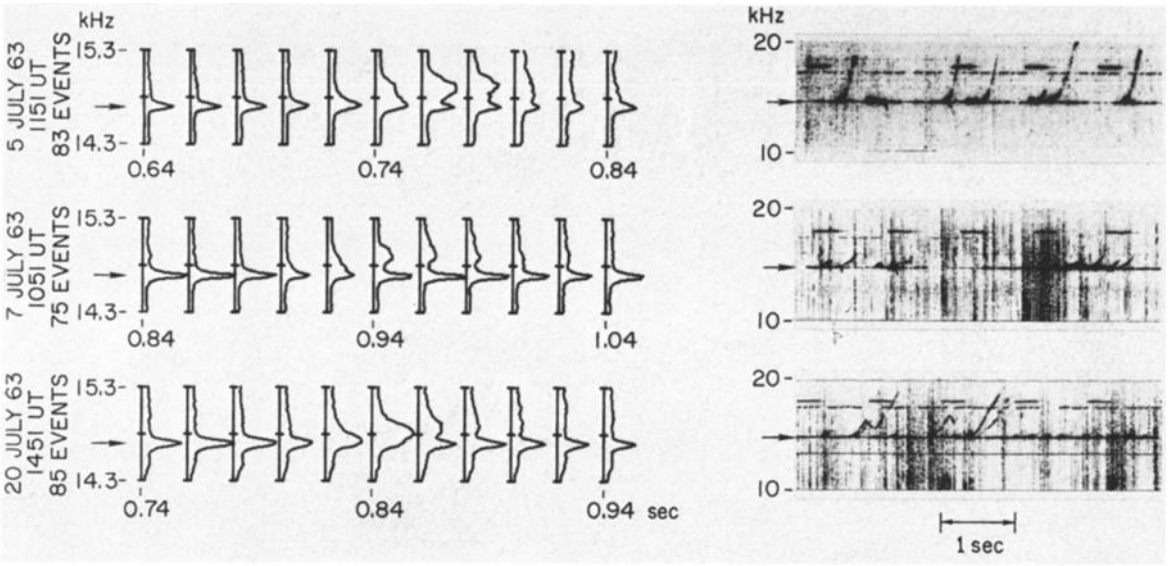

Fig. 4. (Left) Average digital spectra of ASE's triggered by NAA; the number of events included in each average is indicated. Time is measured from the leading edge of the triggering SI dash. (Right) Analog spectra of several of the events contained in each average. In this and subsequent figures the arrow indicates the frequency of the triggering signal (14.7 kHz for NAA).

signal. This requires knowledge of the time delay along the WM path. Because of the usual multiplicity of available paths, and the overlapping SI signal, this delay is difficult to determine accurately. On each of the three days studied, however, there is a path available that would place the initial appearance of the ASE near the end of the WM pulse. This conclusion seems reasonable in view of the regularity of the initial appearance of the emissions.

The most interesting portion of the averages in Figure 4 is found in the traces preceding the plateau. Consider first, as a reference, the 14.7-kHz peak in the first trace of each set. This peak is the average of the combined SI and WM waves and contains very little, if any, off-frequency emission component. As is expected, it is narrow and fairly symmetric. Subsequent traces, however, show progressive broadening on the high-frequency side of the peaks. In the traces immediately preceding the offset peaks there is clearly some signal present between the transmitted frequency and the plateau. The shape of these traces suggests that the emissions actually begin at the frequency of the transmitted signal and then rise rapidly to a point where the slope may abruptly level off to form a short plateau.

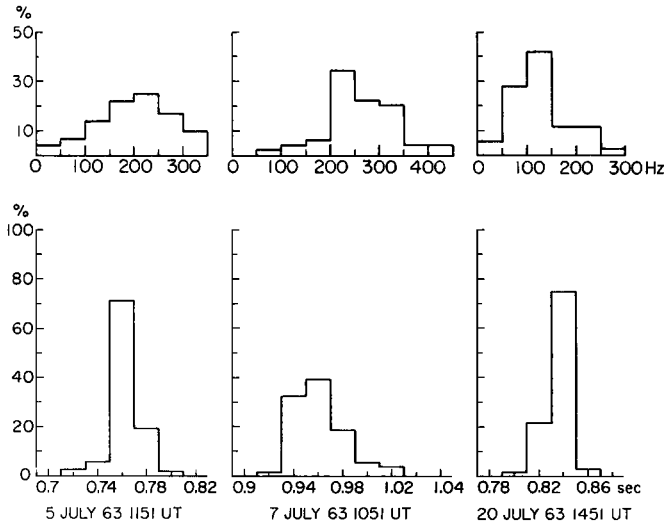

Fig. 5. (Top) Histogram of the spacing (in hertz) above the triggering signal of the maximum emission amplitude. (Bottom) Histogram of the time of occurrence (measured from the leading edge of the triggering SI dash) of the maximum emission amplitude. The number of events included are 73 from July 5, 59 from July 7, and 74 from July 20.

Note that there is no corresponding behavior on the low-frequency side of the 14.7-kHz peak; to at least the level of the background its lower edge retains essentially the same shape throughout the data. This might be expected, since most of the events in these data are rising tones. However, we shall see that falling tones exhibit the same initial behavior.

In the top two spectra of Figure 6 the data of July 5 are separated according to whether the emissions are rising or falling tones. The spectra show that rising and falling tones from the same run display essentially the same initial behavior. Both begin with a broadening on the high-frequency side of the 14.7-kHz peak and develop into an offset plateau. From this point the traces of the two tones diverge: the rising tones persist at the offset frequency for 40 ms or so, while the falling tones begin to decrease in frequency almost immediately.

In the bottom spectra of Figure 6 we see similar behavior in several falling tones from June 10, 1963. At first glance it may appear that broadening first occurs on the low-frequency side, in contrast to the results above. Closer examination, however, shows that the initial broadening of the trace does occur on the high-frequency side at 0.84 s. At 0.86 s the peak has actually risen to 14.725 kHz, and at 0.88 s, when there is considerable broadening on both high- and low-frequency sides, the peak is at 14.75 kHz. The shape of the trace at 0.88 s suggests that the emission, within the 40-ms time window of the analysis procedure, rises from the triggering frequency to a point 50 or 60 Hz higher and then falls rapidly 150 Hz or so; this behavior would account for the fact that broadening is seen on both sides in this trace and only on the high side in the previous trace (recalling that adjacent traces overlap the data by 50%).

This last group of NAA emissions (June 10) has one feature that separates it from the previous data: the entire behavior of

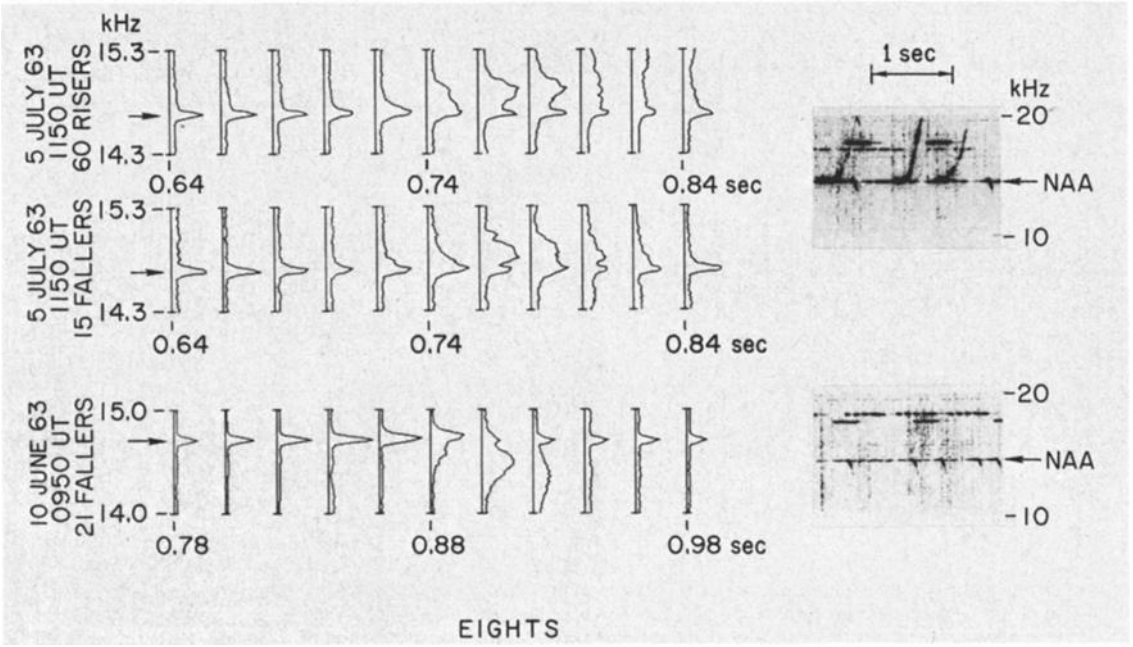

Fig. 6. (Left) Average digital spectra of rising and falling tones. (Right) Analog spectra of several events contained in each average.

the falling emissions, as well as their initial appearance, is very repeatable from event to event. The events of July 5, on the other hand, show considerable variation following the offset peak. When we examine the data from Siple station, we will see a similar effect: short rapidly falling emissions are the most regular in their structure.

The next data to be considered consist of WM signals originating at the Forestport, New York, Omega transmitter and received at Eights in June 1963 and July 1965. The signals were transmitted at a frequency of 10.2 kHz with a radiated power of approximately 100 W. The transmitter is located near $L = 3$.

Figure 7 shows the pulse format tramsmitted by three Omega stations during June 1963. The basic sequence consisted of eight pulses of lengths varying from 0.9 to 1.2 s; all pulses are spaced by 0.2 s. Forestport transmitted alternate pulses of 0.9, 1.1, 1.1, and 1.2 s. Intermediate pulses were transmitted by either Haiku, Hawaii, or Balboa, Panama Canal Zone.

On June 10 the Eights receiver detected only the SI wave from Haiku and the WM wave from Forestport. The WM delay along the Forestport-Eights path was approximately 1.4 s; the Forestport pulses are shown, below the transmitted format, shifted to the right by this amount. Because of this shift, alternate Forestport WM pulses are overlapped at the receiver by the SI pulses from Haiku. As the figure shows, one Haiku pulse arrives nearly simultaneously with the previous Forestport pulse, while the other Haiku pulse arrives about 0.1 s prior to its predecessor. (Previous reports have considered this 100-ms segment to be a portion of the Forestport WM signal [*Carpenter*, 1968; *Diesendorf*, 1972].)

Figure 8 is the average of twenty-two 1.1-s pulses from June 10, 11 of which were overlapped by the SI signal from Haiku. The origin (0.0 s) is the time when the leading edge of the WM

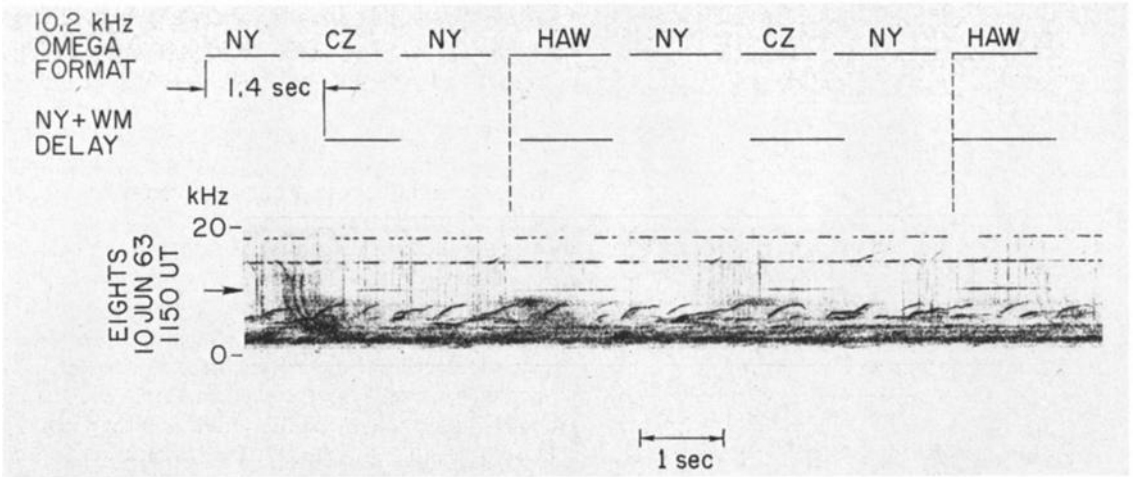

Fig. 7. (Top) Pulse pattern transmitted at 10.2 kHz by Omega stations on June 10, 1963 (NY, Forestport, New York; CZ, Balboa, Panama Canal Zone; HAW, Haiku, Hawaii). (Middle) The NY signal shifted to the right to account for the WM delay between NY and Eights. (Bottom) Spectra of the signal as received at Eights. Note that alternate NY WM pulses are overlapped by the SI pulses from HAW. The CZ pulses are not detected at Eights on this occasion.

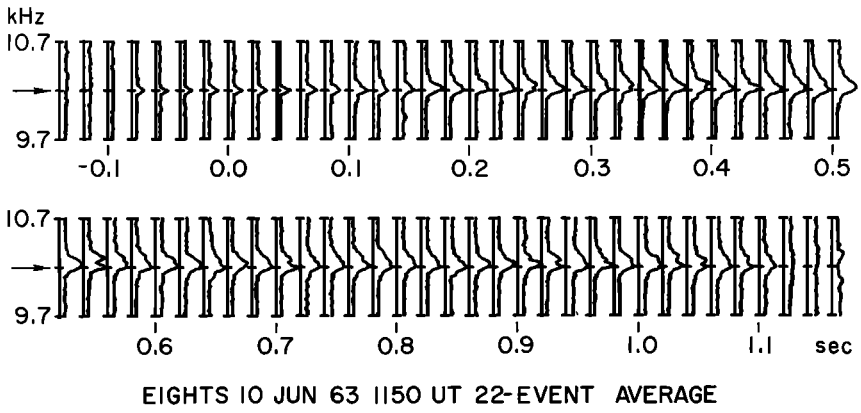

Fig. 8. Average digital spectra of twenty-two 1.1-s NY Omega pulses from June 10, 1963, half of which were overlapped by the SI pulses from HAW. In this and the following figures, 0.0 s designates the time that the leading edge of the transmitted WM signal is received.

pulse should arrive at the receiver. The Haiku pulses were 1.2 s long and arrived approximately 0.1 s prior to the Forestport pulses; the two pulses thus terminated at roughly the same time. This situation is similar to that observed in NAA, where we were also analyzing overlapping SI and WM signals.

The initial traces of Figure 8, from −0.1 to 0.0 s, are the spectra of the Haiku SI signal alone; the traces display the expected narrow and symmetric peaks of an essentially monochromatic tone. The WM signal should arrive at 0.0 s; it is apparently of low initial amplitude, since it has little effect on the spectra for the first 60 ms. At about 0.08 s, however, we begin to notice the same broadening on the high-frequency side of the peak that we observed in the NAA data. This progressive broadening again suggests that the stimulated emission begins at the frequency of the transmitted signal.

By 0.2 s the peak has become about twice as broad as it was originally; this increase is maintained throughout the duration of the pulse. As in the case of NAA, the broadening appears entirely on the high side. The WM signal rarely, if ever, drops below 10.2 kHz prior to the termination of the transmitted pulse.

Examination of individual emissions shows that the initial low-amplitude portion is fairly repeatable from event to event. Subsequent behavior, both in frequency and in amplitude, may be quite irregular. Many pulses appear to be composed of a succession of short (~120 ms) rising tones, most of which do not develop into sustained emissions unless they occur near the end of the transmitted signal. Occasionally, one or more long risers may be triggered prior to the termination of the transmitter pulse. (A clear example of repeated triggering of risers by a single pulse may be seen in the paper by *Helliwell and Katsufrakis* [1974].)

An example of the fluctuations that may occur is given in Figure 9, which shows a single nonoverlapped 1.2-s pulse from July 4, 1965. The amplitude of the minimum at 0.44 is nearly 30 dB below the maximum at 0.96 s. A number of additional local minimums and maximums may also be seen. We should note that these fluctuations do not appear to be very regular, either within a pulse or from pulse to pulse, and are probably of the same type as those described by *Diesendorf* [1972].

The initial frequency behavior of this pulse is particularly interesting. The signal first appears at 10.2 kHz at ~0.2 s, dips in amplitude, reappears somewhat higher in frequency, and continues to rise until reaching its maximum frequency near 0.36 s. The frequency then decreases, returning to 10.2 kHz where the amplitude drops by 15 dB in 40 ms. This rise and fall pattern resembles the initial behavior of the falling tones, described above, that trail most of the pulses in this run (one may be seen near 1.25 s). In the Omega data of June 10 we observed a similar situation: there the predominant trailing tones were risers, and segments resembling the initial portion of risers were often seen within individual pulses. We noted that a few of those internal rising segments succeeded in becoming sustained tones, although most did not. In the present data the internal segments that resemble falling tones always die out as they cross 10.2 kHz; the only falling tones

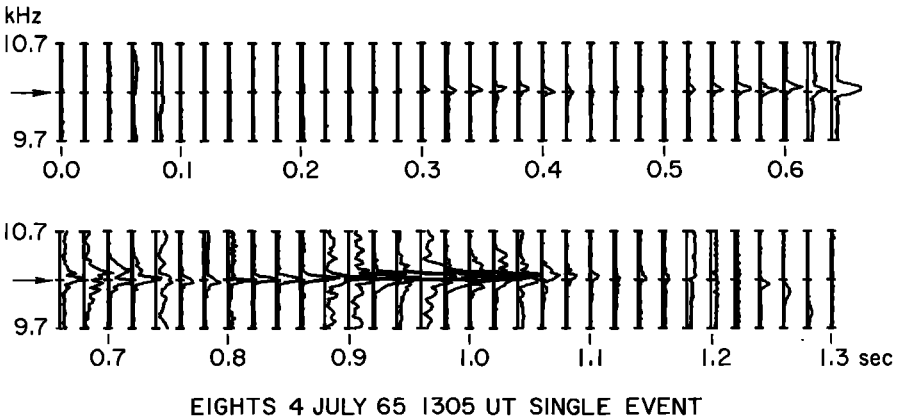

Fig. 9. Digital spectra of a single 1.2-s Omega WM pulse.

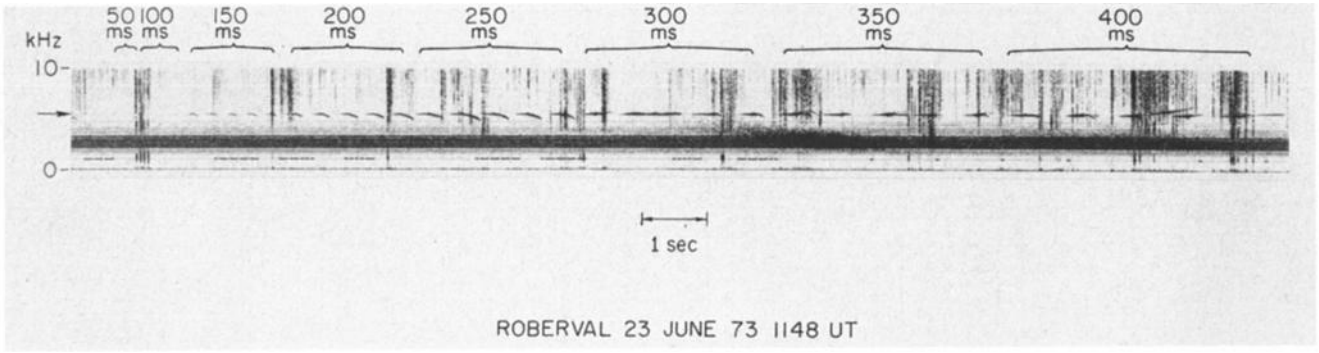

Fig. 10. Analog spectra of a sequence of variable length WM pulses transmitted from Siple, Antarctica, at 5.5 kHz and received at Roberval, Quebec. The length (in milliseconds) of the transmitted pulses is shown at top. Five pulses were transmitted at each length.

that survive are those that cross the triggering frequency after the triggering signal has terminated. The presence of a relatively weak transmitter signal thus appears to interfere in some manner with the development of both rising and falling emissions. For additional examples of the quenching of an emission by another signal, see *Helliwell and Katsufrakis* [1974].

The last set of data to be examined is from the recently installed Stanford VLF transmitter at Siple, Antarctica ($L \approx 4.2$). This installation and some preliminary results of the wave injection experiments have been described recently by *Helliwell and Katsufrakis* [1974]. During the period of observation the transmitter was radiating approximately 400 W at 5.5 kHz. The WM signals were recorded at Roberval, Quebec, Canada.

A portion of the analyzed data is shown in Figure 10. At this time the transmitter was using frequency shift keying between 4.5 and 5.5 kHz (the 4.5-kHz signals were relatively weak and will not be discussed). The length of the pulses at each frequency was varied from 50 to 400 ms in 50-ms steps; 10 consecutive pulses at each length were transmitted, five at each frequency. Note that, in contrast to the NAA and Omega data, there are no interfering SI waves from either Siple or other stations; the analyzed signals are thus entirely WM. Despite the absence of SI waves, however, we still have reference lines produced by locally induced signals at harmonics of the 60-Hz power system; several harmonics are detectable as faint horizontal lines in Figure 10. (See *Helliwell and Katsufrakis* [1974] and *Helliwell et al.* [1975] for a discussion of apparent interactions between the harmonic lines and emissions.)

The digital spectral averages are presented in Figure 11. Individual averages have been computed for each of the eight different pulse lengths. The number of events included in each average is indicated; events obscured by particularly strong

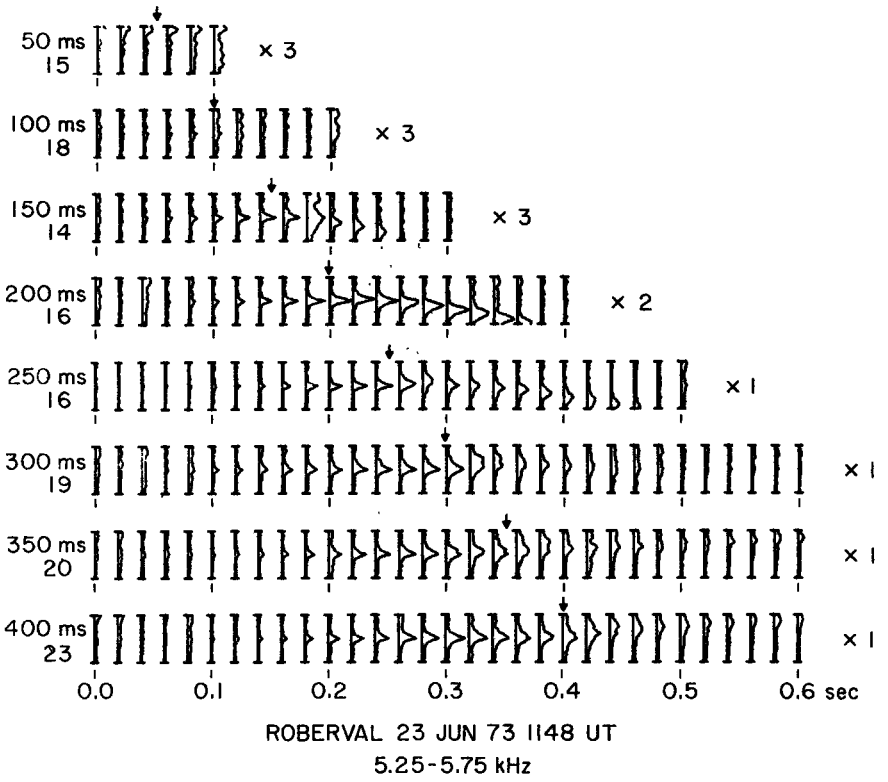

Fig. 11. Average digital spectra of the pulses from Figure 10. The length of the pulse and the number of events included in each average are indicated on the left. The vertical arrows mark the termination of the transmitted pulse. Note that different amplitude scales are used on the first four averages.

spherics have not been included. The leading edges of the received pulses are aligned at 0.0 s, and the different times of termination of the input signal are marked by arrows. Note that different amplitude scales have been used on the shorter pulses.

The shortest pulse (50 ms) is not discernible in the average; a few of the individual pulses were detectable when the background spherics were sufficiently weak, however. The next pulse, 100 ms in length, rises above the average background at about 0.06 s, as do the remaining longer pulses. The signal remains at the transmitted frequency, and there is little or no evidence of off-frequency emissions, although occasional events did appear to give rise to very short-lived fallers.

When the duration of the triggering signal is increased to 150 ms or more, however, nearly every pulse produces an off-frequency emission; the behavior of these emissions changes with the length of the transmitted pulse. Pulses less than 300 ms long usually produce falling tones, whereas longer pulses usually produce risers. Emissions triggered by 300-ms pulses may rise, fall, or simply drift around 5.5 kHz. We should note that the increase in pulse length is not always sufficient to produce risers, often producing only falling tones of increased intensity.

All emissions show evidence of an initial rise in frequency following termination of the input signal. This rise, which ranges from less than 25 Hz in the 150-ms pulses to about 100 Hz for the longest pulses, is followed by a decrease in slope that precedes the final falling or rising phase of the emission. In the 400-ms pulse this decrease results in a plateau at about 5600 Hz, which persists for perhaps 60 ms. This initial

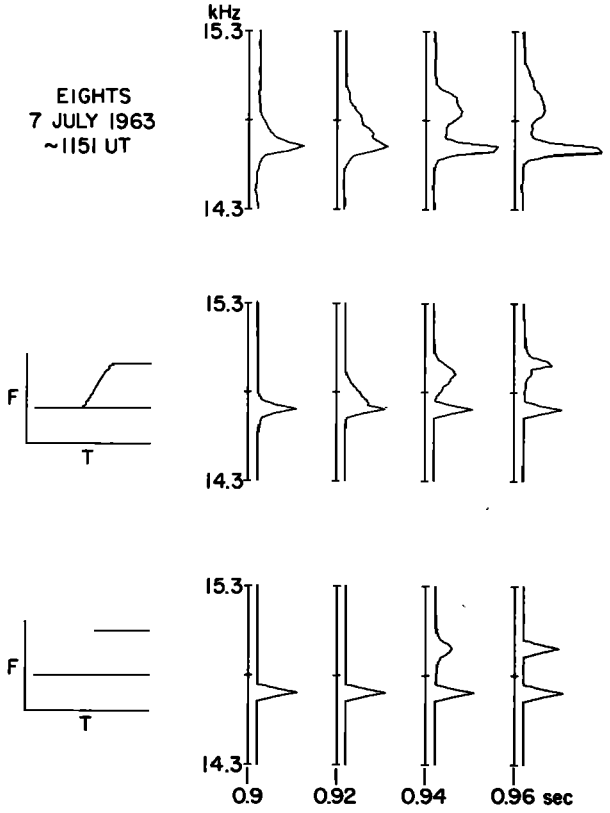

Fig. 12. Comparison of the data of July 7, 1963, with the spectra of two mathematical models of the received signal. In the first model the emission begins at the frequency of the triggering signal and rises smoothly to a point 250 Hz higher, where it levels off. In the second model the emission originates at the offset frequency.

behavior is similar to that of the NAA emissions. The most regular emissions are the fallers produced by the 200-ms pulses, as can be seen from their clean well-defined average. Recall that the most regular NAA emissions were the rapidly falling tones of June 10, 1963.

At this point we should look briefly at the amplitude behavior of the averages. Note that although the amplitude of the shorter pulses continues to increase up to the termination of the input signal, the amplitude of the three longest pulses does not increase significantly past 0.26 s; this behavior indicates that the growth process must saturate at a certain level. Examination of individual pulses shows that the initial growth is typically exponential at a rate of about 125 dB/s [*Helliwell and Katsufrakis*, 1974; *Stiles*, 1974]. Saturation and exponential growth have been predicted by *Helliwell* [1967] and *Helliwell and Crystal* [1973], respectively. These features will be discussed in more detail in a subsequent paper.

In the Siple pulses we see behavior similar to that seen previously in the NAA and Omega data. For pulses less than or equal to 200 ms in length the received signal is very close to the frequency of the transmitted signal. For longer pulses, after 200 ms the high-frequency side of the spectral peak shows evidence of broadening and often considerable irregularity. This behavior indicates that the emission has a tendency to rise but is constrained in some manner to lie within 50 Hz or so of the transmitted frequency. When the injected signal terminates, the emission then continues independently, developing into a sustained rising, falling, or quasi-constant tone. These features again suggest, as in the NAA and Omega data, that the off-frequency emissions actually begin at the frequency of the transmitted signal and are continuous with the stimulated on-frequency emission.

Discussion

In this section we shall check the validity of our principal conclusion and discuss the major features of the data. The suggestion that the emissions actually begin at the frequency of the transmitted signal can first be checked by comparing the spectral averages to the spectra of mathematical test tones. A comparison of the data from June 7, 1963, with the spectra of test signals is shown in Figure 12; the left side of the figure illustrates schematically the frequency-time models used to calculate the test spectra. The test signal consists of two individual signals, both of constant amplitude. One component is on for the duration of the test and maintains a constant frequency; this represents the SI wave that is present in all the averages of NAA data. The second component comes on midway through the test and represents the emission. In the first model, suggested by the digital data, this component begins at the frequency of the triggering signal and rises smoothly to the offset frequency, where it levels off. In the second model the emission begins at the offset frequency, as was suggested by previous studies. Spectra are calculated for a uniform distribution of initial phases between the two components and then averaged. The result is combined with a uniform background (representing the average spheric level) and plotted as shown.

The model in which the emission begins at the triggering frequency clearly reproduces the essential features of the data better. Additional tests show that any model with an emission beginning within $\simeq$30 Hz of the triggering signal will do nearly as well; this is perhaps to be expected, since the analysis filter width is of similar magnitude. This also indicates, unfortu-

nately, that we are approaching the limit of resolution for these data. Since the frequency of the emission changes significantly (~100 Hz) in a time less than 30 ms, we would like to use a time window much narrower than 30 ms. This implies, however, that our frequency resolution will be no better than $(30\ \text{ms})^{-1} \sim 33$ Hz. Thus the strongest statement we can make is that, within the resolution allowed by the data, the emissions begin at the frequency of the injected signal.

We now return to the analog techniques to see if they may be improved sufficiently to yield the same conclusion. The standard analog display may be seen in Figure 4; it covers the range from 10 to 20 kHz, and the gain is high enough to make visible all signals of interest. This procedure unfortunately obscures the details of closely spaced signals. There are two related reasons: first, the high gain setting results in considerable blooming of the scope trace when strong signals, such as the WM and SI waves, are present; second, this blooming, when it is coupled with the small scale size necessitated by the display of 10 kHz across 30 mm of film, effectively obscures a weaker signal that is within 100 Hz or so of a stronger one.

Figure 13 shows a spectrogram that has been processed to minimize these two problems; the scale has been expanded by a factor of 2, and the gain has been reduced. The improvement is immediately apparent. One can now see, again within the resolution (approximately 30 Hz) of the procedure, that the emissions do begin at the frequency of the injected signal: the portion joining the offset plateau to 14.7 kHz is clearly visible. (Note that the ultimately falling and rising tones show identical initial behavior: a sharp rise followed by an abrupt decrease in slope. We should note that the rising tones do not always show a plateau.)

The behavior is typical of the events in this and other runs. In many cases, however, the initial rapidly rising portion is relatively weak. It is not difficult to see how such a weak leading edge, coupled with a peak in amplitude at the plateau, could easily leave the impression that the emission begins at the plateau frequency. The irregular response of the analyzer filters and the frequent presence of spherics would further serve to hide the short rising portion. These features can account for the differences between the results of this paper and those of *Kimura* [1967] and *Lee* [1968].

Next we interpret our findings in terms of a recently developed model of the stimulated emission mechanism [*Helliwell*, 1967, 1970; *Helliwell and Crystal*, 1973]. The observation that all emissions begin at the frequency of the triggering signal and initially rise in frequency is consistent with the model. Emission radiation is assumed to come from transverse currents formed by counterstreaming electrons that have been temporarily phase bunched by the constant frequency triggering signal. Phase bunching occurs all along the path but is maximum at the equator where the inhomogeneity is least. As the phase-bunched electrons move away from the bunching region, they radiate waves at progressively higher frequencies because of the increase in their gyrofrequency. However, their ability to start a self-sustaining oscillation at their radiation frequency may be inhibited by the presence of the triggering wave, which could prevent the stimulated components from producing sufficient phase-bunched current.

Upon emerging from the end of the triggering wave train, these phase-bunched currents radiate waves that are no longer subject to interference from the triggering wave. A self-sustaining oscillation may then begin as described by *Helliwell and Crystal* [1973]. These oscillations may in turn inhibit other new oscillations. The resulting slope (df/dt) of the ASE is a simple function of the position on the field line at which the feedback oscillation takes place [*Helliwell*, 1967, equation (15)]. The slope is zero at the equator. It becomes increasingly positive downstream and negative upstream. Thus for emission locations well downstream from the equator there will be a discontinuous change in slope from the triggering signal to the emission; this may explain the sharp initial rise illustrated by Figure 13.

On the basis of this discussion, we find that ASE's triggered by NAA, with an initial slope of ~10 kHz/s, begin at a point ~1500 km downstream from the equator. Here we assumed that $L = 3.1$ and $f_N = 180$ kHz. The ASE's triggered by the 400-ms Siple pulses have an initial slope of about 3 kHz/s. Assuming $L = 4.3$ and $f_N = 100$ kHz, we find that these emissions begin about 3600 km downstream.

Further development of the mechanism described above requires information not yet available. We need to know the electron distribution function, and the effects of inhomogeneity must be included in the feedback model of *Helliwell and Crystal* [1973]. Should these ideas be correct, new information on the pitch angle distribution of the resonant electrons may be derivable from the slopes of the triggered emissions.

Recent computer simulations by *Nunn* [1974] also predict emissions that begin at the triggering frequency. His calculations, which include the inhomogeneity of the medium, indicate that both risers and fallers should show an initial rise in frequency, as we have seen that they do. (It should be noted that the simulations of *Nunn* [1974] and *Helliwell and Crystal* [1973] are based on fundamentally different physical models, even though they both predict an initial rise in frequency.)

We should now consider why the slope often abruptly levels off and forms a short plateau of nearly constant frequency that precedes the final rising or falling phase. This question is particularly complex because, as equation (15) of *Helliwell* [1967] shows, we expect the constant frequency portion of the emission to be generated at the equator. However, as we just noted above, the initial sharply rising portion appears to come from some distance down the field line. It is difficult to move the region of generation rapidly enough to account for the rapid change in slope.

A possible explanation is that we are actually seeing two

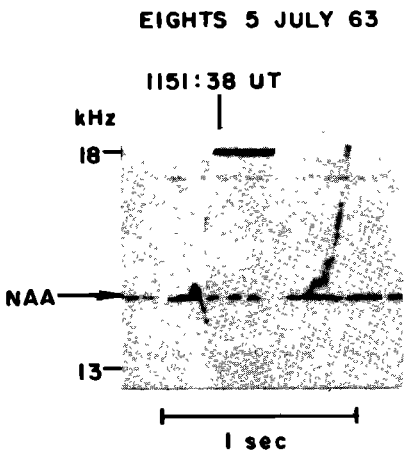

Fig. 13. Expanded analog spectra of two ASE's from the data of July 5, 1963. Note that both emissions begin at the transmitted frequency and show an initial rise.

emissions, one generated downstream and one on the equator. The process may be similar to the triggering of emissions at the upper cutoff of whistlers [*Carpenter,* 1968], where we often see the steep portion of the whistler trigger an emission that begins with nearly constant frequency. In the present case the initial sharply rising portion of the emission, which we assume is generated downstream, corresponds to the whistler. After this emission has risen for several hundred hertz, it may terminate (a possible explanation for the termination is offered below). When it propagates to the equator, it may, like a cutoff whistler, trigger a constant frequency emission. This constant frequency emission can then develop into a rising or falling tone in the manner described by *Helliwell* [1967].

The termination of the sharply rising emission and the enhanced triggering at the plateau may be due to the effect of the sustained wave-particle interaction upon the electron distribution function. At the equator we postulate that the flux of resonant electrons available for wave growth at the transmitter frequency is reduced by scattering during repeated encounters of the same electrons (returned through mirroring) with the waves. We expect this reduced flux to produce a depression in the growth rate of the emissions [*Helliwell and Crystal,* 1973]. At the equator this depression will occur at the transmitter frequency. As the particles move downstream, however, the depression will move to higher frequencies, owing to the increase in the local gyrofrequency. At the region where the rising emission is generated this depression will be located several hundred hertz above the triggering frequency and may account for the termination of the riser. As the short riser propagates back up the field line, it will begin to move out of the frequency range of this depression. When the riser reaches the equator, the growth rate may be increased to the point where retriggering is possible. This mechanism is clearly quite speculative, since it depends on perturbations of the particle flux distribution that have not yet been calculated or observed.

A second possibility is that the rising emission interacts at the plateau with some other weak signal. *Helliwell and Katsufrakis* [1974] give examples of very weak signals, thought to be associated with power line radiation, causing large changes in the slope of emissions triggered by the Siple transmitter. These signals do not necessarily occur at harmonics of the power line frequency but may drift over a range of a hundred hertz or more [*Helliwell et al.,* 1975]. If such a signal is responsible for the plateau, this drift could account for the spread in the plateau frequency. An alternate possibility is that the weak signal at the plateau is caused by a side band instability initiated by the triggering pulse itself [e.g., *Nunn,* 1973, 1974; *Sudan and Ott,* 1971]. We should point out that no evidence of an additional signal at the plateau has been observed. The examples of Helliwell and Katsufrakis, however, show that even a nearly undetectable signal can produce large effects upon much stronger emissions.

CONCLUSIONS

We have applied digital spectral analysis techniques to the study of emissions triggered by three VLF transmitters (NAA, 14.7 kHz, 1 MW; Omega, 10.2 kHz, 100 W; Siple, 5.5 kHz, 400 W). This method has yielded several new results, the most significant of which we list below:

1. Within the resolution of the procedure (~45 Hz, ~30 ms), ASE's begin at the frequency of the transmitted signal.

2. All emissions, regardless of their final slope, initially rise upon leaving the triggering frequency.

3. Emissions triggered by NAA are very repeatable in their initial off-frequency behavior. These emissions may form a short (~40 ms) plateau roughly 200 Hz above the triggering signal.

4. The initial low-amplitude portions of the signals stimulated by Siple and Omega are also fairly repeatable. After the amplitude approaches its peak value and the frequency begins to rise significantly, the behavior may become irregular.

5. Emissions stimulated by the Omega and Siple transmitters rarely drift more than 100 Hz above the triggering frequency before the triggering signal has terminated; this behavior suggests that the relatively weak input signal exercises some control over the much stronger emission.

6. In the one day of Siple data examined in detail the probability of producing a rising emission increases with increasing pulse length. The maximum emission amplitude does not increase past ~260 ms, however.

7. Emissions triggered by all three transmitters show the same basic features; this result indicates that the generation process is relatively independent of transmitter frequency and power.

The results provide a much better definition of ASE's than has previously been available. They should therefore aid in reaching a better understanding of magnetospheric wave-particle interactions. In a subsequent paper we shall further improve the definition by considering in detail the amplitude behavior of stimulated emissions.

Acknowledgments. The authors' work was supported in part by the Office of Naval Research, under contract NONR N00014-67-A-0112-0012, and in part by the Air Force Office of Scientific Research, under grant F4462-72-C-0058. Collection of the data was supported in part by the Office of Polar Programs of the National Science Foundation, under grant GV-28840X, and in part by the Atmospheric Sciences Section of the National Science Foundation, under grant GA-32590X. We are indebted to T. L. Crystal for critical comments on the manuscript.

The Editor thanks R. L. Dowden and R. Gendrin for their assistance in evaluating this paper.

REFERENCES

Bergland, G. O., A guided tour of the fast Fourier transform , *IEEE Spectrum, 6,* 41, 1969.

Carpenter, D. L., Ducted whistler mode propagation in the magnetosphere; A half-gyrofrequency upper intensity cutoff and some associated wave growth phenomena, *J. Geophys. Res., 73,* 2919, 1968.

Carpenter, D. L., K. Stone, and S. Lasch, A case of artificial triggering of VLF magnetospheric noise during the drift of a whistler duct across magnetic shells, *J. Geophys. Res., 74,* 1848, 1969.

Cousins, M. D., A computer program for dynamic spectrum analysis applied to VLF radio phenomena with examples and comparisons to rayspan results, *Tech. Rep. SU-SEL-71-056,* pp. 33–42, Radioscience Lab., Stanford Electron. Lab., Stanford Univ., Stanford, Calif., 1971.

Diesendorf, M. O., Amplitude variations in artificially stimulated VLF emissions, *Nature, 236,* 56, 1972.

Gendrin, R., Gyroresonant wave-particle interactions, in *Solar-Terrestrial Physics/1970,* part 2, edited by E. R. Dyer, p. 236, D. Reidel, Dordrecht, Netherlands, 1972.

Helliwell, R. A., *Whistlers and Related Ionospheric Phenomena,* pp. 296–299, Stanford University Press, Stanford, Calif., 1965.

Helliwell, R. A., A theory of discrete VLF emissions from the magnetosphere, *J. Geophys. Res., 72,* 4773, 1967.

Helliwell, R. A., Intensity of discrete VLF emissions, in *Particles and Fields in the Magnetosphere,* edited by B. M. McCormac, pp. 292–301, D. Reidel, Dordrecht, Netherlands, 1970.

Helliwell, R. A., and T. L. Crystal, A feedback model of cyclotron in-

teraction between whistler mode waves and energetic electrons in the magnetosphere, *J. Geophys. Res., 78,* 7357, 1973.

Helliwell, R. A., and J. P. Katsufrakis, VLF wave injection into the magnetosphere from Siple station, Antarctica, *J. Geophys. Res., 79,* 2511, 1974.

Helliwell, R. A., J. Katsufrakis, M. Trimpi, and N. Brice, Artificially stimulated very-low-frequency radiation from the ionosphere, *J. Geophys. Res., 69,* 2391, 1964.

Helliwell, R. A., J. P. Katsufrakis, T. F. Bell, and R. Raghuram, VLF line radiation in the earth's magnetosphere, submitted to *J. Geophys. Res.*, 1975.

Hinich, M. J., and C. S. Clay, The application of the discrete Fourier transform in the estimation of power spectra, coherence, and bispectra of geophysical data, *Rev. Geophys. Space Phys., 6,* 347, 1968.

Kimura, I., On observations and theories of the VLF emissions, *Planet. Space Sci., 15,* 1427, 1967.

Kimura, I., Triggering of VLF magnetospheric noise by a low-power (~100 watts) transmitter, *J. Geophys. Res., 73,* 445, 1968.

Lasch, S., Unique features of VLF noise triggered in the magnetosphere by Morse code dots from NAA, *J. Geophys. Res., 74,* 1856, 1969.

Lee, B. G., Spectrum analysis of VLF emissions, *Tech. Rep. SU-SEL-68-081,* p. 19, Radioscience Lab., Stanford Electron. Lab., Stanford Univ., Stanford, Calif., 1968.

Nunn, D., The sideband instability of electrostatic waves in an inhomogeneous medium, *Planet. Space Sci., 19,* 1141, 1973.

Nunn, D., A self-consistent theory of triggered VLF emissions, *Planet. Space Sci., 22,* 349, 1974.

Rife, O. C., and G. A. Vincent, Use of the discrete Fourier transform in the measurement of frequencies and levels of tones, *Bell Syst. Tech. J., 49,* 197, 1970.

Stiles, G. S., Controlled VLF experiments, in *Proceedings of the NATO Advanced Study Institute on ELF-VLF Radio Wave Propagation,* D. Reidel, Dordrecht, Netherlands, 1974.

Sudan, R. N., and E. Ott, Theory of triggered VLF emissions, *J. Geophys. Res., 76,* 4463, 1971.

Welch, P. D., The use of fast Fourier transform for the estimation of power spectra: A method based on time averaging over short, modified periodograms, *IEEE Trans. Audio Electroacoustics, 15,* 70, 1967.

(Received April 15, 1974;
accepted October 23, 1974.)